Chapter 1

Introduction

1.1 Objective

Isolation between the closely spaced antenna elements in a low profile (specifically microstrip and printed antennas) multi-element antenna structures is the most critical factor to determine the performance of the antenna systems. Isolation is evaluated in terms of coupling coefficient which is a ratio of power coupled to one port with the power input to another port. Low coupling coefficient leads to the poorly coupled (heavily isolated) antenna ports while high coupling coefficient indicates heavily coupled (poorly isolated) antenna ports. Mutual coupling in antenna elements has undesirable effects like,

i. Distortion in the radiation pattern and
ii. Changes the input impedance of the antenna elements, therefore, increases the mismatch which overall reduces the efficiency of the antenna system.

The space wave effect which includes far field radiations and near-field radiations and surface wave effect (lowest order mode of the surface wave always propagate even in thin low permittivity dielectric substrate as it has zero cutoff frequency [Garg *et al.* (2001)]) are responsible for mutual coupling in multi-element antenna systems designed using microstrip technology. Shorted antennas like an inverted-F antenna (IFA) and planar inverted-F antenna (PIFA) are the preferred choices for small footprint antenna systems owing to their compact geometry [Anguera *et al.* (2013)]). Mutual coupling in such antenna elements is more severe because of the flow of sufficient current through the antenna ground plane. On the integration of the antenna system with the device

chassis along with other electronic components (like battery, amplifier, LCD), antenna isolation severely affected. Therefore, investigation of the efficient isolation enhancement techniques suitable for various applications is in demand.

1.2 Coupling in Multi-element Antenna Structures

1.2.1 Antenna Array

Antenna arrays are usually employed for better directivity and side lobe level reduction. Microstrip antenna arrays gained popularity due to its low profile nature. Beam scanning applications like radar and satellite widely employed microstrip phased arrays. An array designed with microstrip technology are having a drawback of narrow bandwidth. Bandwidth is increased by using thicker substrate. However, surface wave effect becomes stronger for the substrate thickness satisfying Equation 1.1 [Garg *et al.* (2001)], which in turn increases the mutual coupling among the antenna elements. The large physical separation between the antenna elements decreases the coupling at the cost of increasing the array size. Moreover, grating lobe appears for the element spacing greater than half wavelength [Balanis (2003)]. Mutually coupled antenna elements in microstrip phased arrays also leads to the problem of scan blindness in which effectively no power is transmitted and received by the array [Pozar and Schaubert (1984)].

$$\frac{h}{\lambda_0} \geq \frac{0.3}{2\pi\sqrt{\varepsilon_r}} \tag{1.1}$$

where h is the substrate thickness, λ_0 is free space wavelength, and ε_r is the substrate dielectric constant.

The effect of the coupling on the performance of antenna array depends on the antenna type, inter-element spacing of array elements, feeding mechanisms, and array

scan volume. The mutual coupling in antenna arrays is characterized in terms of mutual impedance. Mutual coupling and hence the mutual impedance behaves differently in transmit and receive mode of the antenna array [Allen and Diamond (1966)]. Mutual impedance is conventionally defined in transmit mode of the antenna array as Equation 1.2 [Kraus (1988)].

$$Z_{mn} = \frac{\text{induced open circuit voltage of antenna } m}{\text{terminal current of antenna } n} \tag{1.2}$$

where m and n denote the two elements of an antenna array. For the receiving mode, the direction of incident EM wave and the effect of the terminal load have to be accounted. The receiving mutual impedance and its measurement procedure are presented in [Hui (2004)]. Mutual coupling between the microstrip patch antenna elements are theoretically calculated using transmission line model [Krowne and Sindoris (1980), Krowne (1980), Lil and Capelle (1984)], cavity model [Malkomes (1982), Penard (1982), Penard (1983)] and moment method [Pozar (1982)].

1.2.2 Multiple-input multiple-output (MIMO) Antenna

MIMO is a cutting-edge wireless technology that improves the spectral efficiency and channel capacity of a wireless link without the need of additional bandwidth and transmitted power. The history of the MIMO technology dates back to 1984 with the publication of Winters [Winters (1984)]. Later, a number of efforts have been made by many researchers to better understand the MIMO system [Paulraj and Kailath (1994), Foshchini (1996), Raleigh and Jones (1999)]. MIMO system utilizes more than one antenna elements at both ends of the wireless link. Therefore, with n_T transmit and n_R receive antennas the number of the channel between the transmitter and receiver become n_T x n_R. Spatial multiplexing is used to transmit several independent data streams using multiple antenna elements at the same frequency, thereby increasing the

spectral efficiency. A single data stream gets n_R channels, and thus even in an urban environment rich in multipath fading, the signal is effectively received as all the channels would not get fading dip at the same time. For the better signal reception, following antenna diversity [Vaughan and Andersen (1987)] methods are used at the receiving terminal:

i. **Spatial diversity –** multiple antenna elements occupy separate locations on the device.

ii. **Polarization diversity –** the antenna(s) provide dual orthogonal polarizations.

iii. **Pattern/Angle diversity –** directional antennas discriminate over angle space.

A combining technique is applied to the received signals by choosing the strongest branch signal or using all the branch signals and combine them as depicted in Figure 1.1. The various signal combining techniques are as:

i. **Selection combining:** It is a linear combining method of selecting an instantaneously stronger signal.

ii. **Switched combining:** It works by switching to the other antenna when the signal from one antenna falls below a certain threshold.

iii. **Equal-gain combining:** it works by adding the signals from the two antennas when they are co-phased.

iv. **Maximal ratio combining:** It is the most complicated one, using weights at each signal such that the output will be a sum of their signal-to-noise ratios.

A M x N element MIMO antenna system is shown in Figure 1.2. The shown system is mathematically modeled using Equation 1.3.

$$Y = HX + n \tag{1.3}$$

where Y = output signal vector, X = input signal vector, H = channel matrix, and n = additive white Gaussian noise (AWGN) vector.

The channel matrix H is defined as in Equation 1.4 [Winter (1987)],

$$H = \begin{bmatrix} h_{11} & \text{L} & h_{1M} \\ \text{M} & \text{O} & \text{M} \\ h_{N1} & \text{L} & h_{NM} \end{bmatrix} \tag{1.4}$$

where, $h_{rt} = S_{ij}$, $r = 1,..., N$ and $t = 1,..., M$ and S_{ij}, $j = 1, ... , M$; $i = M + 1 ... , M + N$ is the complex transmission coefficient between the j^{th} transmit antenna and the i^{th} receive antenna. The channel capacity of M x N MIMO system is given by Equation 1.5 [Foschini and Gans (1998)].

$$C = log_2 \left\{ \left| \boldsymbol{I} + \frac{SNR}{M} \boldsymbol{H}\boldsymbol{H}^{\dagger} \right| \right\} \text{ bits/s/Hz} \tag{1.5}$$

where, $\boldsymbol{I} = M$ x N identity matrix and $\boldsymbol{H}^{\dagger}$= conjugate transpose of the channel matrix.

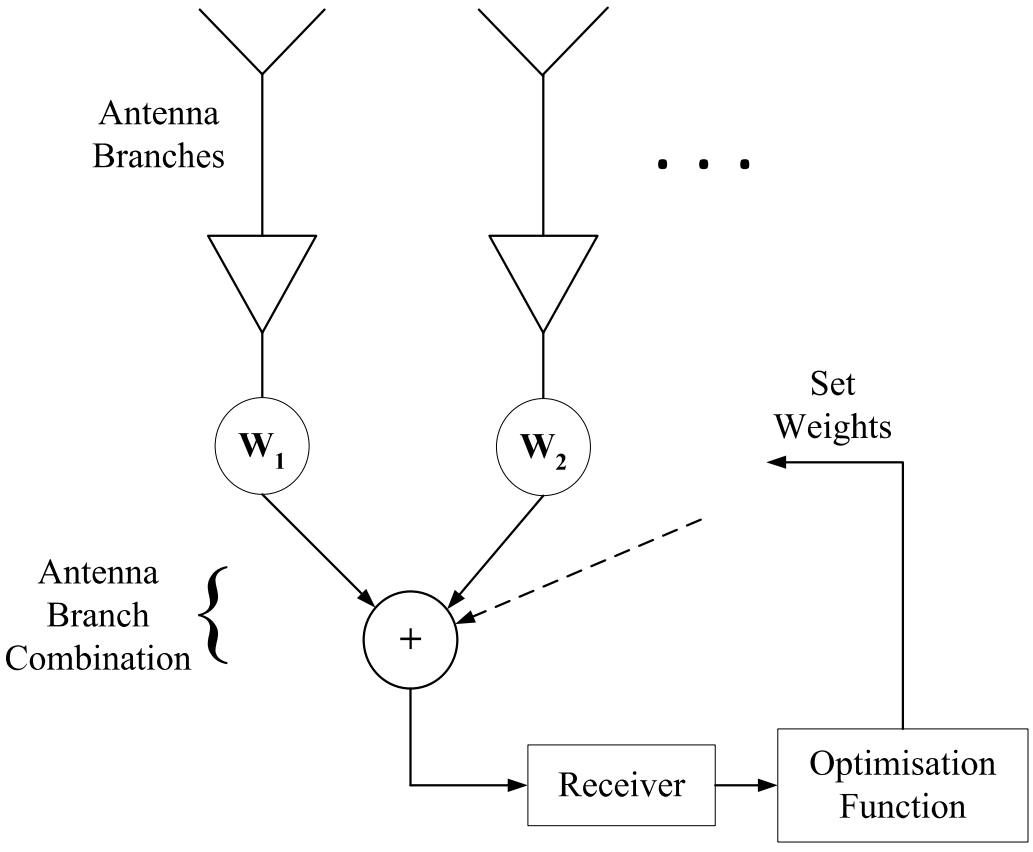

Figure 1.1: Signal combining on receiving uncorrelated fading branches [Vaughan and Andersen (2003)].

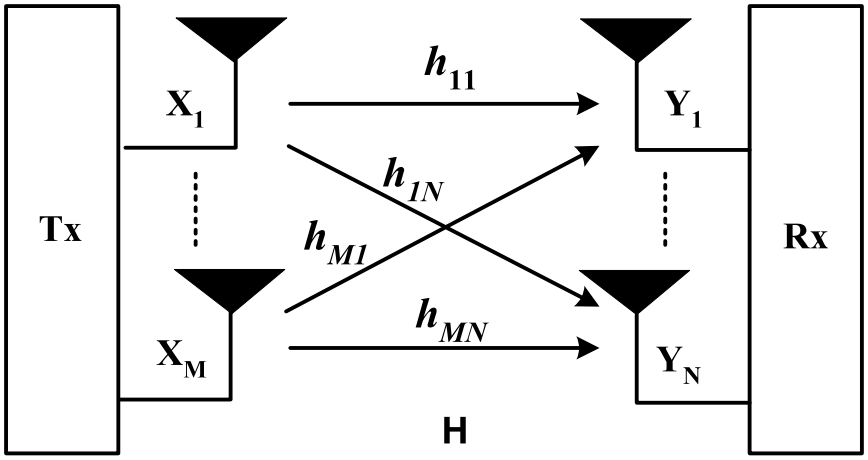

Figure 1.2: *M* x *N* MIMO antenna system.

The channel capacity of the MIMO systems not only depend on the signal-to-noise ratio at the receiver but also on the channel correlation [Mcnamara *et al.* (2000)]. The mutual coupling between the antenna elements on each side of the MIMO system led to the higher correlation between channel and causes loss of channel capacity [Fletcher *et al.* (2003)]. To account for the correlation, envelope correlation coefficient (ECC) is calculated for MIMO system performance and diversity among the antenna elements is determined by the diversity gain (DG).

1.2.2.1 Envelope Correlation Coefficient (ECC)

ECC is calculated either using far field pattern or *S*-parameters data. The ECC for a two element MIMO system is calculated using the far-field approach as given in Equation 1.6 [Vaughan and Andersen (1987)].

$$\rho_e = \frac{\left| \iint_{4\pi} [\vec{F_1}(\theta,\phi) \bullet \vec{F_2}(\theta,\phi)] d\Omega \right|^2}{\iint_{4\pi} \left| \vec{F_1}(\theta,\phi) \right|^2 d\Omega \iint_{4\pi} \left| \vec{F_2}(\theta,\phi) \right|^2 d\Omega} \tag{1.6}$$

where $\vec{F_i}(\theta,\phi)$ is the far field radiation pattern of the antenna system with port *i* excited and all other ports matched terminated. The symbol '●' denotes the Hermitian product.

The far-field approach is more realistic but tedious in the calculation as the radiation pattern data is needed at every frequency. A straightforward relation of envelope correlation coefficient and the *S*-parameters of the two port MIMO antenna system is derived in [Blanch *et al.* (2003)] and given as Equation 1.7.

$$\rho_e = \frac{|S_{11}^* S_{12} + S_{21}^* S_{22}|^2}{\left(1-(|S_{11}^2| + |S_{21}^2|)\right)\left(1-(|S_{22}^2| + |S_{12}^2|)\right)} \tag{1.7}$$

The *S*-parameters based approach is easy in calculation both experimentally and numerically. The above relation is further extended to calculate the correlation between any two ports (*i* and *j*) of the *N* port antenna system [Thaysen and Jakobsen (2006)] as given in Equation 1.8.

$$\rho_e(i,j) = \frac{\left|\sum_{n=1}^{N} S_{i,n}^* S_{n,j}\right|^2}{(1-\sum_{n=1}^{N} S_{i,n}^* S_{n,i})(1-\sum_{n=1}^{N} S_{j,n}^* S_{n,j})} \tag{1.8}$$

The *S*-parameters based ECC calculation assumed the antenna system as a lossless structure and is in a uniform scattering environment. In a practical scenario, these assumptions do not hold good. ECC calculation using *S*-parameters has uncertainty in results if the antenna elements have low radiation efficiency and the correlation of the losses is not known [Hallbjörner (2005)]. However, in the mobile application, *S*-parameters approach is utilized for quick low-cost characterization of the systems.

1.2.2.2 Diversity Gain

The diversity performance is measured in terms of diversity gain, a time-averaged quantity that can be defined as the improvement in time-averaged signal-to-noise ratio (SNR) from the combined signal from a diversity antenna system, relative to the SNR from one single antenna in the system [Vaughan and Andersen (1987)]. Apparent diversity gain of a two-antenna system is related to the correlation coefficient ρ_e by the approximate expression given in Equation 1.9 [Schwartz *et al.* (1965), p. 474].

$$DG = 10\sqrt{1 - |\rho_e|^2} \tag{1.9}$$

The factor 10 in the above equation is the maximum apparent diversity gain. The square root term is the correlation efficiency, which indicates the reduction in diversity gain due to the correlation between the antenna elements. Effective diversity gain (EDG) can be calculated by multiplying the apparent diversity gain by the antenna radiation efficiency [Kildal *et al.* (2002)].

1.2.3 Repeater Antenna

Repeaters are installed as a cost-effective alternative of the base station to improve the cell coverage and enhancing wireless connectivity in dead spots. The capacity and coverage enhancement of universal mobile telecommunication services (UMTS) by the radio repeater is thoroughly discussed in [Rahman and Ernström (2004), Patwary *et al.* (2005)]. A repeater system is presented in Figure 1.3, and it consists of repeater unit (amplifier and pre/post processing units), donor antenna (receiving antenna) and a server antenna (transmitting antenna). Donor antenna looks towards the base station and receives signal in the downlink path while retransmitting the amplified signal towards the base station in uplink path. Conversely, server antenna retransmits the amplified signal towards the end user in downlink path and receive the signal from the end user in

the uplink path [Marzuki *et al.* (2006)]. The radio frequency (RF) repeaters are classified as,

i. **On-frequency repeaters:** has same frequency for receive and retransmit the signal
ii. **Frequency shifting repeater:** has a different frequency for receive and retransmit signal

The on-frequency repeaters are preferred over frequency shifting repeater due to its low cost. However, the amplifier gain and hence, the maximum coverage range is limited by the isolation between the donor and server antenna. Poor isolation has following effects on the repeater system performance [Luis *et al.* (2008)]:

i. Magnitude and phase errors in the repeated signal,
ii. Magnification of high undesired spurious signals,
iii. Instability and self-oscillation in the amplifier (reamplification of its own signal coming from feedback path), and
iv. The mismatch between the antennas and the amplifier.

The need for antenna isolation is quantified and repeater system stability criteria are discussed in [Slingsby and McGeehan (1995)] and are presented as follows:

Considering the Figure 1.3, various notations are:

G_{df}: Donor antenna forward gain (towards base station) (dB)

G_{dr}: Donor antenna reverse gain (towards server antenna) (dB)

G_{sf}: Server antenna forward gain (towards the end user) (dB)

G_{sr}: Server antenna reverse gain (towards donor antenna) (dB)

G_a: amplifier gain (dB)

A_r: attenuation in repeater unit (dB)

A_p: path loss considering isotropic donor and server antenna (dB)

SM: safety margin (dB)

A_s: donor and server antenna isolation (dB)

These parameters are related as in Equation 1.10.

$$A_s + A_p + A_r - G_{dr} - G_{sr} > G_a + SM \tag{1.10}$$

and the repeater total forward gain is given by Equation 1.11.

$$G_t = G_a + G_{df} + G_{sf} \tag{1.11}$$

The antenna isolation must be higher than the gain of the amplifier by an amount equal to the safety margin of 10–15 dB to ensure unconditional stability in the repeater [3GPP release 6 (2004)].

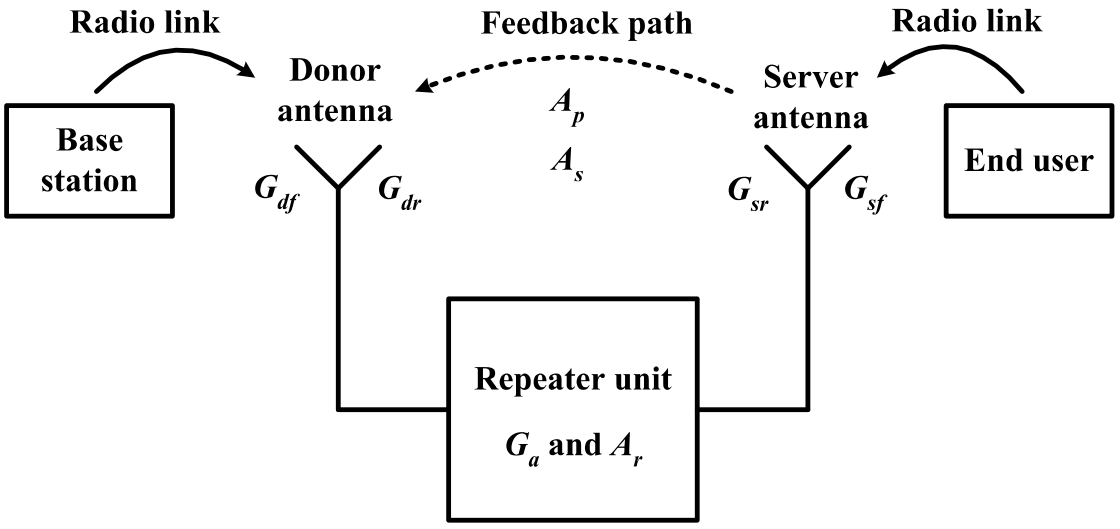

Figure 1.3: Schematic of a repeater system.

1.3 State-of-the-Art Review of Isolation Enhancement Techniques

Reduction of mutual coupling between antenna elements always fascinates the research community. Therefore, a number of isolation enhancement techniques have been proposed in the literature. In the present section, the state-of-the-art review of the various isolation enhancement techniques and their potential effect on antenna characteristics is presented.

1.3.1 Decoupling Network

A decoupling network made up of lumped elements and the microstrip lines are placed between the input ports of the coupled antenna elements. Such a network decouples the input ports by counterbalancing the coupling between the antenna elements. In [Andersen and Rasmussen (1976)], the necessary conditions to completely eliminate coupling and scattering between the antenna element was discussed. It was concluded that the mutual impedance must be reactive so that power orthogonality between antenna elements could be achieved. A network of transmission line was proposed to connect at the feed ports of the coupled antennas to reduce the effect of mutual coupling between them. Such a decoupling network of transmission lines and reactive component was used between the feeding ports of the coupled printed monopole antennas separated by $0.069\lambda_0$ at 2.45 GHz in [Chen (2008)]. The use of decoupling network deteriorates the port matching and hence, an impedance matching section was also added. The decoupled antennas radiated in different directions and thus pattern diversity was realized. The isolation increased from 3 dB to 10 dB in the entire band of interest (2.4–2.5 GHz) with the peak isolation value of 30 dB. A miniaturized version of the monopole antennas was also presented with reduced antenna separation of $0.040\lambda_0$ at 2.45 GHz. Measured isolation of better than 10 dB was observed for the entire band with the peak value of 20 dB at 2.46 GHz.

1.3.2 Neutralization Line

The concept of using neutralization line to enhance the isolation was first proposed in [Diallo *et al.* (2006)] between the PIFA elements operating at a different frequency band (DCS1800 and UMTS). In this method, a suspended link was created by directly connecting the driven element with the coupled element at the same position. In this method of isolation enhancement, the two antennas were electromagnetically coupled due to the direct connection; however, isolation improves because of the cancellation of direct and coupling current at the coupled antenna. Two versions of the techniques were presented by connecting the neutralization line between the shorting and feeding strip of the antennas to create frequency independent current divider and frequency dependent current divider, respectively. The concept of neutralization line was further extended to be used for PIFA elements operating at similar frequencies [Diallo *et al.* (2008)]. The isolation becomes better than −17 dB with neutralization line between the shorting strip and better than −18 dB with neutralization line between the feeding strip compared to −8 dB isolation without using neutralization line. The utilization of neutralization line was further explored in [Wang *et al.* (2014)a]. In this work, a neutralization line network was proposed for the three port MIMO antenna system for 2.4 GHz band. Mutual coupling reduced by 16 dB between all pairs of port, and become better than −15 dB throughout the band. The edge to edge separation was kept $0.006\lambda_0$ between the antenna elements. Furthermore, Zhang and Pedersen [Zhang and Pedersen (2016)] achieved high isolation in wideband of 3.1–5 GHz in the UWB spectrum. Higher than 22 dB isolation was achieved in the entire frequency range, however, bandwidth gets reduced by the wideband neutralization line. The neutralization line has a disadvantage of narrow bandwidth and the difficulties associated with the selection of the location to

connect the neutralization line that requires a complete analysis of current distribution on the radiator make this technique unappealing.

1.3.3 Ground Resonator

In this method of decoupling, a resonator was connected to the ground plane and positioned in between the coupled antennas. This resonator traps the coupled ground current and prevents it to reach the neighboring antenna. This technique is effective for the printed monopole and PIFA antennas. One use of this technique was investigated by Lee *et al.* [Lee *et al.* (2012)]. They used meander line resonator along with the shorted parasitic line to improve isolation between the folded monopole antennas operating at WCDMA (1.92–2.17 GHz), WiMAX (2.3, 2.5 GHz), WLAN (2.4 GHz), and UWB (3.1–10.6 GHz) bands. Measured isolation of better than 17.2 dB is obtained in all the operating frequency bands. In the same year, Li *et al.* [Li *et al.* (2012)] achieved better than 23 dB isolation between the two monopole antennas operating at UWB frequency band using resonator connected to the ground plane. Recently, in [Xun *et al.* (2017)], a dual-band isolation enhancement structure consisting of inverted-L shaped metal strips along with the spiral line was connected to the ground in between the two PIFA elements. Isolation improvement of 11.5 dB at 2.4–2.483 GHz band and 7.2 dB at 5.25–5.9 GHz band was achieved. The presented structure has an advantage of better isolation enhancement performance in dual-band and compact in size.

1.3.4 Defective Ground Structure (DGS)

In this method of isolation enhancement, defects are created in the ground plane by cutting the slots/slits that prevent the flow of the current in the ground plane between the two neighboring antenna elements. Such a defected ground structure behaves like band stop filter and its characteristics are the function of the geometrical parameters.

The isolation enhancement capability of various DGS geometries like slitted pattern [Chiu *et al.* (2007) and Li *et al.* (2009)], bent slits [Li *et al.* (2012)], pair of slot [Shin and Park (2007)], U-shaped slot [Zhou *et al.* (2012)], dumb-bell like slot [Zhu *et al.* (2009)], spiral open slot [Jiang *et al.* (2012)a], square ring [Anitha *et al.* (2014)], and S-shaped periodic DGS [Wei *et al.* (2016)] were explored in the literature. However, the presence of DGS degrades the antenna radiation pattern due to the leakage of radiations through the DGS structure, and hence, deteriorates the antenna front-to-back ratio. Moreover, due to its resonant nature, DGS need to be combined with other isolation enhancement techniques in multiband antenna structures. Some of the works presenting the combination of DGS with other isolation enhancement techniques are reviewed as follows:

1.3.4.1 DGS with Different Antenna Orientation

In [Kim *et al.* (2008)], the two wideband antennas operating in the frequency range 2.3–5.9 GHz are placed obliquely to generate orthogonal current paths. Better than 10 dB isolation was achieved in all the frequency bands of interest at the low-frequency side. A λ/4 slot is etched on the ground plane to block the flow of current at 5 GHz and 7 dB isolation improvement was achieved at 5 GHz.

1.3.4.2 DGS with Neutralization Line

In [Wang and Du (2014)], better than 15 dB isolation was obtained between the antenna elements in a quad-antenna system operating in 1.7–2.74 GHz. A pair of folded T-shaped slots and three neutralization lines were used to decouple the antenna elements. Recently, a combination of neutralization line and ground slot were exploited to decouple closely spaced multi-band antenna elements proposed for USB dongle

applications and better than 14 dB isolation was achieved by Singh *et al.* [Singh *et al.* (2016)].

1.3.4.3 DGS with Ground Resonator

In [Shoaib *et al.* (2015)], multiband MIMO antenna elements were isolated by better than 15 dB in all frequency bands of interest by employing ground slot along with the inverted-L shaped ground resonator.

1.3.5 Resonator Between Radiators

Microstrip and printed antenna elements are coupled due to the flow of surface wave and direct coupling path in the antenna near field. However, for the thin substrate, the effect of surface wave is not appreciable. To overcome the effect of the direct coupling path, a resonator is placed between the coupled antenna elements, so that the scattered wave from the resonator provide indirect coupling path. The resonator is designed in a way that the amplitude of the signal coming from the indirect path is equal to the direct path signal and the two signal add destructively. With this approach, a significant reduction in mutual coupling is achieved. Moreover, the inserted resonator should not deteriorate the antenna radiation characteristics. This approach was firstly presented in [Minz and Garg (2010)] to decouple the PIFA elements placed as a separation of 0.09λ. Simulated coupling coefficients reduced to −24.8 dB from the −3.28 dB by using the shorted patch with air substrate as resonator between the PIFA elements. Several other resonator like U-shaped microstrip, I-shaped microstrip, slotted meander line, meander line, and parallel metal strips were studied and analyzed to improve isolation in microstrip patch antennas in [Farsi *et al.* (2012)], [Ghosh and Parui (2013)], [Alsath *et al.* (2013)], [Ghosh *et al.* (2016)], and [Sun and Cao (2017)], respectively. A significant

improvement in isolation was achieved by these various resonators in the desired frequency bands without affecting the antenna radiation characteristics.

1.3.6 Other Miscellaneous Techniques

Some other miscellaneous techniques reported in the literature for the antenna isolation enhancement are as follows:

1.3.6.1 Radio Frequency Choke

RF choke is an important circuit component used to prevent the RF signal to pass through the circuit. A RF choke constructed using microstrip lines and via holes was used in between the MIMO antenna elements in [Ga *et al.* (2013)]. The use of RF choke improved the isolation and return loss characteristics simultaneously. The presented antenna system was working at LTE band 13 (746–787 MHz), and isolation became better than 10 dB in the entire band with a 20 dB improvement at the center frequency of the band.

1.3.6.2 Branch Line in Conjugation with the Suspended Line

In [Bae *et al.* (2010)], the combination of branch line along with the suspended line was proposed to achieve 12–15 dB isolation in between PIFA elements in the LTE700 band. It is shown that the inclusion of branch line significantly improved the isolation.

1.3.6.3 Orthogonal Antenna Placement along with Metal Wall

Isolation between the donor and server antennas of a repeater antenna system operating in the 3G band (1.92–2.5 GHz) was increased to more than 80 dB by placing the antenna elements orthogonally on opposite sides of the metallic zig and utilized inverted-U shaped metallic wall in [Lee *et al.* (2010)]. A 3-dB attenuator is also employed to improve the isolation by 10 dB in the low-frequency side of the desired band. The comparative study of the various shapes of the metallic wall like I, inverted-

L, and inverted-U was studied and it was found that inverted-U shape has the best performance in terms of isolation and sidelobe level in the entire band of interest. It was shown that metallic wall is capable of improving isolation by 10 dB, and height of the wall significantly affects the isolation characteristics of the proposed repeater antenna system.

1.3.6.4 Neutralization Line and Decoupling Network

In [Chen (2014)], multiband planar antennas separated by $0.1\lambda_0$ corresponding to the lowest operating frequency were decoupled using the neutralization line connected to the ground plane between the coupled antennas. A tunable capacitor was connected at the center of the line to tune the isolation bandwidth. Better than 10 dB measured isolation was reported at all the operating frequencies. The proposed decoupling structure did not affect the matching characteristics of the antennas and hence no additional matching network was required.

1.3.6.5 Near-field Cancellation Method

This method of decoupling the antenna elements was proposed by Song and Sarabandi for the repeater antenna system [Song and Sarabandi (2012)]. In this method, an end-fire array of two-element transmit antenna was utilized. A receiving antenna was placed at the null plane created in between the transmit array and mutual coupling reduced to −86 dB at the design frequency.

1.4 State-of-the-Art Review of Metamaterial/Metasurfaces Based Isolation Enhancement Techniques

The metamaterial is the periodic artificially engineered material that can manipulate the propagation of the incident electromagnetic wave. The response of the metamaterials towards the incident EM wave can be molded by varying the design parameters of the

resonator forming the metamaterial unit cell. The planer form of the metamaterial is termed as metasurface. The potential of metamaterial/metasurface for mutual coupling reduction has been explored in the literature along with their many other applications. A state-of-the-art review of metamaterial/metasurface based isolation enhancement techniques is presented below:

1.4.1 Electromagnetic Bandgap Material

Electromagnetic bandgap structure based isolators were extensively explored in the literature. Initially, mushroom-like EBG structures were developed [Sievenpiper *et al.* (1999)]. In [Yang and Samii (2003)], mushroom type EBG structures were used between the patch antenna array working at 5.86 GHz and 8 dB reduction in mutual coupling was observed in the measured results. An elongated mushroom EBG structure was used in [Coulombe *et al.* (2010)] to decouple patch antennas placed in E-plane and H-plane coupled configuration and its efficacy was compared with the perfect electric conductor (PEC) block and conventional mushroom EBG block. Furthermore, the use of mushroom type EBG was also investigated for isolation enhancement in the waveguide-slot antenna array, and isolation improvement of 10 dB was reported in [Ebadi and Semnani (2014)]. In some of the works, a wall of mushroom type EBG cells was utilized between the antenna elements and sufficiently high isolation was obtained [Qiu *et al.* (2012) and Zhai *et al.* (2015)a]. However, these mushroom-type EBG structures require metallic via which increases the electric loss and also not a very attractive structure from the point of view of manufacturing. Therefore, the planar EBG structure was developed and explored as an isolator. One such planar EBG was utilized between the printed dipole antenna array designed for 4.2 GHz in [Abedin and Ali (2005)], and 13 dB reduction in coupling was obtained. Similarly, planar EBG was used to decouple patch antenna array operating at 3 GHz in [Rajo-Iglesias *et al.* (2008)], and

10 dB improvement in isolation was achieved. The potential of planar EBG was also explored for the millimeter wave antenna array with the dielectric resonator as radiator and 13 dB reduction in mutual coupling was reported in the frequency range of 57–64 GHz in [Al-Hasan *et al.* (2015)].

1.4.2 Metamaterial Absorber

The metamaterial absorber structure attenuates the energy of the incident electromagnetic waves. A number of such structure were developed in the microwave to optical frequency ranges [Landy *et al.* (2008), Pitchappa *et al.* (2014), Wang *et al.* (2015)a, Wang *et al.* (2015)b]. These structures have shown the application of mutual coupling reduction by decreasing the space wave effect between the antenna elements. A linear array of the metamaterial absorber unit cell was utilized by Lee and Lee [Lee and Lee (2011)] to decouple two coplanar printed loop antennas operating at 2.45 GHz, and 10 dB isolation enhancement was achieved at the operating frequency. Thereafter, the isolation enhancement property of these structures was explored in [Yoon *et al.* (2012) and Lee *et al.* (2012)] for the WCDMA (1.92–2.17 GHz) repeater antenna systems. In these works, transmit and receive antenna were separated and placed in the back-to-back configuration. The presence of metamaterial absorber unit cells in the vicinity of the antennas enhanced the isolation by 10 dB in the desired band. A similar work by Kim *et al.* [Kim *et al.* (2013)] reported 20 dB isolation enhancement in the WCDMA band. In [Wei *et al.* (2014)], a metamaterial absorber wall was used in between the two dual polarized antennas and 10 dB isolation improvement was noticed in the wideband of 1.7–2.2 GHz. The results were compared with the metal wall that provided 7 dB isolation enhancement in the entire band, and hence the proposed absorber wall proved a more efficient way to decouple the antenna elements in the presented configuration.

1.4.3 Split Ring Resonator (SRR)

Split ring resonator is the most basic structure explored to achieve negative permeability. Its application for isolation enhancement was explored in the literature. Lee *et al.* [Lee *et al.* (2010)] achieved approximately 20 dB isolation improvement at 3.5 GHz between the two MIMO antenna elements using SRR array structure. However, the proposed 3-D implementation of the SRR unit cell requires via to connect the top and bottom layers of the SRR which increased the fabrication complexity. In the same year, Bait-Suwailam *et al.* [Bait-Suwailam *et al.* (2010)] achieved 25 dB isolation improvement between two monopole antennas separated by $0.125\lambda_0$ at 1.24 GHz. The vertically installed strips of single-negative magnetic metamaterial designed using SRR geometry was used as an isolator. The space wave was prevented to propagate from the driven element to the coupled element using these metamaterial strips. Furthermore, the inclusion of more number of such strips increased the isolation, however, this ultimately increases the overall volume of the presented antenna array. Furthermore, in [Park and Lee (2011)], dual-band PIFA elements in MIMO configuration were isolated using slit and SRR cells on the ground plane. SRR cells were bringing mutual coupling down to −20 dB in the United State Personal Communication Services (USPCS) band (1.850 GHz–1.990 GHz). In [Khan *et al.* (2014)], single SRR cell was placed between the patch element to decouple four-element MIMO antenna array operating at 2.45 GHz ISM band, and coupling reduction of 7 dB was achieved.

1.4.4 Complementary Split Ring Resonator (CSRR)

Complementary split ring resonator is generally designed in the antenna ground plane that traps the energy of the propagating surface wave between the antenna elements. In [Bait-Suwailam *et al.* (2010)], two CSRR units are combined with a slot that improved the bandwidth and suppression for 5 GHz microstrip patch antennas. 10 dB isolation

improvement was reported with the element spacing of $0.25\lambda_0$. Later on, the slot combined CSRR were used in [Qamar *et al.* (2014) and Shafique *et al.* (2015)] to decouple two-element microstrip phased array. These works used CSRR unit cells in between patch as well as on the ground plane. In [Yem *et al.* (2012)], the two patch antennas are connected by a CSRR loaded transmission line acting as a band stop filter that provided better than 20 dB isolation in the desired LTE band of 2.30–2.39 GHz with the peak isolation of 41.84 dB at 2.36 GHz. However, the efficacy of the proposed structure was not discussed in the case of the absence of any decoupling structure. Further, in [Ramachandran *et al.* (2016)], isolation was improved in a four-port collocated MIMO antenna using CSRR. The CSRR reverses the coupling current polarity between the coupled antenna and provided 6.5 dB improvement in port isolation.

The SRR and CSRR were together explored for isolation enhancement in [Tang *et al.* (2010)]. SRR array was placed between the patch elements along with CSRR array in the ground plane. The SRR and CSRR in combination formed a composite metamaterial and coupling reduction of 9.07 dB was achieved at 5.82 GHz.

1.4.5 Other Miscellaneous Techniques

1.4.5.1 Metamaterial Substrate

In [Hafezifard *et al.* (2016)], two closely spaced ($0.073\lambda_0$) meandered patch antennas designed with center frequency of 5.5 GHz (frequency band: 5.1–5.9 GHz) were isolated by using a substrate containing elliptical-SRR in between the radiator and the ground plane and isolation enhancement of 15 dB was reported at the center frequency. Further improvement of 4 dB was observed in the isolation by using SRR array in between the radiators. However, the inclusion of such an SRR substrate increased the

thickness of the antenna array and the alignment of two substrate layers has to be taken care of seriously during fabrication.

1.4.5.2 Frequency Selective Surface (FSS) Superstrate

In [Akbari *et al.* (2017)], FSS superstrate was used above the two-element patch antenna array consisting of circularly polarized elements with the center to center spacing of $0.5\lambda_0$ at 30 GHz. The operating bandwidth of the array was 27–33.5 GHz, and 10 dB isolation improvement was observed in the entire band using FSS superstrate.

1.4.5.3 Metamaterial-inspired Resonator with Ground Resonator

In [Hsu *et al.* (2011)], 3-layered metamaterial inspired resonator was placed between the radiator of the two-element MIMO antenna array working at 2.37–2.98 GHz. 20 dB isolation bandwidth of 2.52–2.73 GHz (8%) was obtained. Along with this, a T-shaped resonator was connected in the ground beneath the metamaterial resonator that improved the 20 dB isolation bandwidth to 19.3% relative to the center frequency.

1.4.5.4 Metamaterial Insulator

A metamaterial based channel isolator that acts as a shield between the coupled antennas was proposed to decouple patch antennas separated by $0.1\lambda_0$ in [Buell *et al.* (2007)] and 40 dB reduction in mutual coupling was observed. The metametarial insulator blocks the propagation of EM energy at its boundary. Such a metamaterial insulator was also utilized to isolate transmit and receive antenna in the repeater antenna system in [Sarabandi and Song (2011)].

1.4.5.5 Mantle Cloaking Method

In this method of decoupling the antenna elements were covered by the metasurface cloak so that the closely spaced antenna elements become invisible to each other. The method was first proposed in [Bernety and Yakovlev (2015)] to decouple strip dipole

antennas and later on to decouple microstrip-fed printed monopole antenna in [Bernety *et al.* (2015)]

1.5 Summary of the Literature Review

The effect of mutual coupling between antenna elements on the performance of multi-element antenna systems like antenna array, MIMO antenna, and repeater antenna has been discussed. The state-of-the-art review of a number of decoupling techniques was presented. The pros and cons of these decoupling techniques were also discussed. To overcome the associated disadvantages of these decoupling techniques, advanced techniques based on metamaterial/metasurface were utilized. Metamaterial/metasurface are the engineered electromagnetic materials whose electric and magnetic properties can be molded by changing the shape parameters. Various such structures like split ring resonator (SRR), complimentary split ring resonator (CSRR), electromagnetic bandgap material (EBG), and absorbers have been presented as an isolator in the literature and state-of-the-art review of these isolators was discussed in detail.

1.6 Motivation Behind the Present Thesis

After the extensive state-of-the-art review presented in previous sections, identification of the following research gap motivates to work towards this thesis:

i. Isolation enhancement by restricting the surface wave propagation between the microstrip antenna elements is well reported in the literature. However, the techniques suitable for the compact antenna structure like PIFA in which the space wave effect are the dominant cause of coupling (instead of surface wave effect) are not well addressed.

ii. Isolation (~15 dB) between the antenna elements is easily achieved by utilizing space/pattern diversity, particularly at high operating frequencies. However, the

isolation characteristics deteriorate drastically by integrating the antenna in the actual device chassis due to the coupling from other components. To compensate for this effect, it is always better to have additional isolation between antenna elements.

iii. Metamaterial/metasurfaces have the potential to reduce the coupling. EBG structures are well utilized to reduce the surface wave effect. Metamaterial absorber and the cross-polar converter may provide an edge over other isolation enhancement techniques by manipulating the space wave effect between the antenna elements.

iv. A number of metamaterial absorbers are designed particularly for X-band and above frequencies. The compact and ultra-thin metamaterial absorber unit cells for low frequencies with multiband absorption characteristics are in great demand.

v. The top layer of the metamaterial/metasurface consists of the resonator which acts as a frequency selective surface. Analytical modeling of basic single band resonators like a loop, patch, and cross are addressed in the literature. An analytical model of the multiband resonators is also necessary to get a good insight into the resonance phenomenon.

1.7 Scope and Structure of the Thesis

This thesis investigates some of the metamaterial absorber structures in which the basic resonator geometries like closed ring resonator (CRR) and patch are embedded in a single unit cell. Ultrathin polarization-insensitive wide-angle dual-band and quad-band metamaterial absorbers are realized using this resonator. The simulated response of the absorber is validated experimentally. Transmission line model (TLM) is developed for

the presented dual-band absorber. A variant of the presented metamaterial unit cell is then utilized to improve port isolation in a four-port MIMO antenna system.

The thesis is organized into six chapters. Chapter 1 discussed the isolation requirement in multi-element antenna systems like microstrip antenna arrays, multiple-input multiple-output (MIMO) arrays, and on-frequency repeater antennas. The state-of-the-art review of various isolation enhancement techniques like defected ground structure (DGS), neutralization line, ground resonator, resonator between radiating elements, metal wall, near-field cancellation method, and their combinations are also discussed. The isolation enhancement techniques based on metamaterial are emerging nowadays. Based on the literature review some research gaps are identified that motivated to work towards the present thesis. Finally, the scope and structure of the thesis are discussed.

Chapter 2 presents a dual-band metamaterial based microwave absorber. The proposed absorber is polarization-insensitive with wide-angle performance.

Chapter 3 presents the analytical model of the absorber structure presented in chapter 2 using transmission line method (TLM) to get a good insight into the resonance phenomenon.

Chapter 4 presents a polarization insensitive, wide-angle quad-band absorber by utilizing a variant of electric resonator presented in chapter 2 in 2x2 array configuration as a single unit cell.

Chapter 5 presents a four-port MIMO antenna with high port isolation for 5 GHz WLAN access point application. The cause of coupling between various antenna pairs is identified. Isolation in the antenna ports is improved by placing a finite array of asymmetrical metasurface that responds differently to the TE and TM polarized incident

wave. The effect of the isolator structure on the antenna radiation characteristics and MIMO/diversity performance is evaluated. The low value of envelope correlation coefficient justifies the suitability of the proposed structure for MIMO application.

Chapter 6 briefly concludes the major contributions and summarizes the presented work. The scope for the future work on this topic is also discussed.

Chapter 2

Metamaterial-based Polarization-insensitive Wide-angle Dual-band Microwave Absorber

2.1 Introduction

Conventional microwave absorbers [Salisbury (1952), Fante and McCormack (1988), Naito and Suetake (1971), Toit (1994), Sugimoto *et al.* (1999), Park *et al.* (2000)] need to be replaced in the applications that require lightweight, low profile and low-cost absorbing materials. Such applications include mutual coupling reduction in antenna arrays (discussed in section 1.4 of the previous chapter), radar cross section reduction [Zhang *et al.* (2014)], stealth technology [Iwaszczuk *et al.* (2012)], electromagnetic compatibility [Li *et al.* (2015)], sensors [Liu *et al.* (2010)a], thermal emitter [Liu *et al.* (2011)b], spectroscopy and imaging [He *et al.* (2011)], microwave-to-infrared signature control [Jiang *et al.* (2011)b], and many more. The requirement of having the alternatives of conventional microwave absorbers led to the development of electromagnetically engineered absorbers popularly known as metamaterial absorber. Metamaterial absorbers suitably fit in these applications with the added advantage of frequency tunability over a wide frequency range by just varying the design parameters. Polarization-insensitive nature and wide-angle performance are the desired characteristics of such absorber structures.

Several metamaterial absorber structures with near unity absorption in the upper GHz frequency range to terahertz and infrared frequency ranges are presented in the literature [Landy *et al.* (2008), Wen *et al.* (2009), Cheng and Yang (2010), Zhu *et al.* (2010), Tao *et al.* (2010), He *et al.* (2011), Pitchappa *et al.* (2014), and Wang *et al.* (2015)]. Designing the structure with the small footprint for low GHz frequency range